Pediatr Radiol (1996) 26: 852–860

Suvimol Chirathivat Hill
Bonita M. Damaska
Maria Tsokos
Constance Kreps
Roscoe O. Brady
Norman W. Barton

Radiographic findings in type 3 b Gaucher disease

Received: 22 August 1995
Accepted: 12 December 1995

S. C. Hill (✉) · B. M. Damaska
Diagnostic Radiology Department,
Warren Grant Magnuson Clinical Center,
National Institutes of Health, Building 10,
Room 1 C-660, 10 Center DR MSC 1182,
Bethesda, MD 20892–1182, USA

M. Tsokos
The Laboratory of Pathology,
Warren Grant Magnuson Clinical Center,
National Institutes of Health, Bethesda,
Maryland, USA

C. Kreps · R. O. Brady · N. W. Barton
The Developmental and Metabolic
Neurology Branch, National Institute of
Neurological Disorders and Stroke,
National Institutes of Health, Bethesda,
Maryland, USA

Abstract The purpose of this paper is to describe the radiographic findings in type 3 b Gaucher disease, a chronic neuronopathic form of the illness with severe systemic manifestations. Between 1980 and 1985 17 consecutive patients were evaluated with radiography of the chest, long bones and spine, CT of the head and chest, abdominal sonography, and MRI of the head, abdomen and spine. Clinical manifestations were severe, and led to death from hepatic, pulmonary or cardiac failure in nine patients. Type 3 b Gaucher disease shares the same spectrum of radiographic findings observed in type 1 disease, but the systemic manifestations are more severe. Pulmonary infiltrates, thoracic lymph node enlargement, vertebral compression fractures and osteonecrosis of the long bones occur much more frequently in patients with type 3 b disease.

Introduction

Gaucher disease is an autosomal recessive illness caused by deficient activity of the enzyme glucocerebrosidase [1]. This results in accumulation of glucocerebroside in the lysosomes of macrophages [2]. Most radiologists are familiar with the radiographic findings of type 1, non-neuronopathic, Gaucher disease. This is the most common form, and was previously called the "adult" type. Although this phenotype is panethnic, it is more frequent in Ashkenazi Jews. The frequency of type 1 disease is approximately 1 in 100000 in the Caucasian population. However, among Ashkenazi Jews the frequency is much higher and is estimated to be about 1 in 1500. Types 2 and 3 Gaucher disease, severe forms of the illness, are both rare, with an incidence of less than 1 in 100000 live births, and are characterized by involvement of the central nervous system (CNS).

Two clinically distinct groups of patients with type 3 Gaucher disease have recently been delineated and are designated as type 3 a and 3 b [3–5]. Type 3 Gaucher disease (subacute or chronic neuronopathic or "juvenile form") presents in infancy, childhood, adolescence or adulthood and is clinically heterogeneous. Type 3 b is an early-onset form with severe systemic involvement and static or slowly progressive CNS disease. Most patients show abnormal horizontal eye movements as their sole neurologic abnormality, and death usually occurs in adolescence due to systemic disease. Type 3 a, on the other hand, is a later-onset form characterized by severe progressive CNS disease.

Over the past 15 years, we have evaluated 17 patients with type 3 b Gaucher disease. Early recognition of this

aggressive phenotype of Gaucher disease, for which there is now effective therapy [6, 7], may be facilitated by awareness of the radiographic abnormalities.

Materials and methods

Seventeen patients with type 3b Gaucher disease were identified among the children referred to the Developmental and Metabolic Neurology Branch of the National Institute of Neurological Disorders and Stroke for diagnostic evaluation from 1980 to 1995. The study population included 14 boys and three girls, whose ages ranged from 2 to 15 years. Disease severity was assessed radiographically in each patient with radiographs of the chest, long bones and spine, CT of the head and chest, and MRI scans of the brain, abdomen, knees, and spine. Color Doppler ultrasound of portal venous flow was also performed. The imaging studies obtained in each patient varied over time in accordance with available technology and clinical indications (Tables 1, 2). Autopsy findings were available for comparison with imaging studies in three patients.

Abdominal unenhanced MRI was performed with T1- and T2-weighting using a 0.5-T unit (Vista; Picker International, Cleveland, Ohio). Contiguous transaxial 10-mm-thick sections were obtained through the entire liver and spleen. The motion artifact suppression technique (MAST) was used for all T2-weighted images. The volumes of the liver and spleen were measured in each patient by a previously described method [8]. Sagittal T1-weighted and short tau inversion recovery (STIR) sequences were obtained through the thoracolumbar spine using a surface coil. For the brain, sagittal T1-weighted, transaxial multiecho, and transaxial IR sequences were used.

Images of the abdomen were reviewed for the presence of intraabdominal masses, lymph node enlargement and areas of altered signal intensity in the liver or spleen. Images of the spine were evaluated for the presence or absence of fat within the marrow and for compression fractures of the vertebral bodies. Brain images were reviewed for the presence of atrophy or altered signal intensity.

Unenhanced CT of the chest was performed using an Imatron scanner. Slices 6 mm thick were obtained at 6-mm intervals. Slices 3 mm thick at 12-cm intervals were also made through the chest using a high-resolution technique with an exposure time of 200 ms per slice. The images were evaluated for changes in the lungs and intrathoracic lymph nodes.

Results

Radiographic findings

All 17 patients with type 3b Gaucher disease exhibited significant, and frequently severe, clinical and radiographic abnormalities early in life (Tables 1, 2).

Thorax

Chest radiographs were obtained in 17 patients and were abnormal in 11. Abnormalities included an enlarged thymus ($n = 4$), paratracheal and hilar lymphadenopathy ($n = 3$) and bilateral pulmonary interstitial infiltrates ($n = 10$) (Fig. 1). Six patients had ultrafast CT of the chest. The CT scan was abnormal in five patients, each of whom had an abnormal chest radiograph. The abnormalities included axillary lymphadenopathy ($n = 2$) (Fig. 2a), a large thymus ($n = 4$), interstitial lung disease ($n = 5$), scattered areas of atelectasis ($n = 1$), a ground glass appearance of the lung parenchyma ($n = 1$) (Fig. 2b) and enlargement of the azygos vein ($n = 2$) (Fig. 2c).

Long bones and spine

Long bone radiographs were obtained in 16 patients; 14 showed abnormalities. The degree of abnormality ranged from minimal changes limited to osteoporosis or Erlenmeyer flask deformity to moderate changes manifested by marrow expansion or cystic changes with intact cortical bone. Severe changes included the above abnormalities with cortical interruption (Fig. 3), bone compression or fractures. Bilateral medial cortical erosion of the proximal humerus was noted in eight patients (Fig. 4). Three of these patients also showed erosions of the lateral cortices.

Radiographs of the cervical, thoracic and lumbar spine were obtained in all 17 patients. Eleven had fractures of the vertebral bodies. Two had a single fracture; nine had multiple fractures. None of the patients had evidence of spinal cord compression. Severe gibbus deformity due to the collapse of multiple vertebral bodies was noted in two patients (Fig. 5). Seven patients had MRI scans of the spine and all showed homogeneously decreased signal intensity on the T1-weighted spin echo sequences suggesting a non fatty marrow.

Abdomen

Seventeen abdominal sonograms and seven MR scans showed marked hepatomegaly in all but one patient. One patient had ascites. In two other patients, the contour of the liver was lobular. A few hyperintense nodules were noted on MRI of the liver in patient 11 [9] (Fig. 6); they were hypoechoic on the abdominal sonogram (Table 2). These lesions were confirmed to be regenerating nodules at autopsy. Two patients had enlarged azygos and hemiazygos veins (Fig. 2c, 6). Eleven patients had undergone partial or total splenectomy. One patient with an intact spleen had multiple splenic infarcts on MRI (Fig. 7) that were shown on CT to be partially calcified. Four of the seven patients who had organ volume measurements had intact spleens (patients 13–15 and 17). In each case, the spleen was massively enlarged (19–98 times normal). None of the abdominal MRI studies revealed retroperitoneal lymphadenopathy, Color Doppler examination of seven

Table 1 Clinical and radiographic findings

Patient no.	Age/sex	Death	At age	Cause	CT head	MRI head	Chest film	Chest CT
1	8/M				Min. atrophy	Min. atrophy	Paratracheal, hilar mediastinal lymphadenopathy	
2	15/M	Yes	18 y	Hepatic failure, bleeding varices			Normal	
3	6/M	Yes	8 y 11 m	Bleeding varices	Normal		Normal	
4	8/M				Normal	Normal	Normal	
5	15/M	Yes	16 y 6 m	Cor-pulmonale	Normal		Min. infiltrate	
6[a]	15/F	Yes	15 y 4 m	Cor-pulmonale, bleeding varices	Min. atrophy		Min. infiltrate	
7	4/M	Yes	5 y 9 m	Brainstem bleeding			Prominent thymus, Min. infiltrate	
8	13/M	Yes	15 y	Bleeding varices			Normal	
9[b]	6.5/M	Yes	6 y 10 m	Cardiac involvement	Min. atrophy		Normal	
10	7/M	Yes	8 y 11 m	Bleeding varices	Normal		Diffuse infiltrate	
11[c]	8/M	Yes	9 y 9 m	Hepatic failure, abdominal hemorrhage		Min. atrophy	Large thymus, adenopathy, lung infiltrate	Same as CXR with bilateral axillary lymphadenopathy
12	9/M					Abnormal signals	Large thymus, adenopathy, lung infiltrate	Same as CXR with bilateral, axillary lymphadenopathy
13	3/M					Normal	Subsegmental atelectasis LLL, RLL	Large thymus, atelectasis, ground glass upper lung
14	10/F					Normal	Lung infiltrate	Interstitial lung disease prominent thymus
15	6/M					Normal	Normal	Normal
16	9/M					Normal	Interstitial fibrosis	RUL, lingular: fibrosis
17	2/F						Perihilar infiltrate	

[a] Autopsy findings: brain, nodular accumulation of Gaucher cells perivascularly in subcortical white matter; lung, abundant Gaucher cells in interstitium, heart, myocardium infiltrated with Gaucher cells as well as cranial lymph nodes

[b] Autopsy findings: brain, minimal hydrocephalus, Gaucher cell infiltration in leptomeninges, subarachnoid and Virchow-Robin spaces; Gaucher cell infiltration in thymus, alveolar spaces of lungs and myocardium

[c] Autopsy findings: brain, minimal gliosis of molecular layer and white matter with rare perivascular Gaucher cells; minimal Gaucher cells in thymus

patients showed no evidence of reversal of portal venous flow, although two of these patients had signs of cirrhosis as suggested by large azygos and hemiazygos veins on CT and MRI.

Brain

CT or MRI of the brain were performed in 13 patients (CT 5, MRI 6, CT and MRI 2). Four had minimal cerebral atrophy. One patient with a history of an anoxic brain injury had abnormal signal intensity in the right frontal and left parietal white matter on MRI.

Table 2 Clinical and radiographic findings (continued)

Patient no.	Vertebral fractures	Abnormalities on long bone X-Ray	Liver MRI/ ultrasound	Liver volume in ml (fold enlargement)	Spleen	Spleen volume in ml (fold enlargement)
1	Plana: T6	Severe	Enlarged		Removed	
2	Partial: T4, T6, T10	Moderate	Enlarged, ascites		Removed	
3	Plana: T6	Severe	Enlarged		Very large spleen subcapsular hematoma	
4	Plana: T5, T8 Partial: T9–10, T12, L1–5	Severe	Enlarged, lobular contour		Removed	
5	None	Severe	Enlarged		Removed	
6[a]	Plana: T6, T9, T11–12, L2 Partial: L3	Moderate	Enlarged		Removed	
7	Not done	Not done	Enlarged		Partial resection infarcts, calcification	
8	Plana: T3–4, T9 Partial T8, L2	Severe	Markedly enlarged		Removed	
9[b]	None	None	Minimally enlarged		Enlarged	
10	Plana: T6, T9 Partial: T10–12, L1, L5	Severe	Heterogeneously enlarged		Removed	
11[c]	Partial: T7–L3	Mild	Liver nodules on MRI/sonogram, large azygos vein	532 (1.2)	Subtotal splenectomy	441 (12.8)
12	Plana: T6, T12/ kyphosis Partial: L1–2, L4	Severe	Heterogeneous, lobular contour, large azygos/ hemiazygos veins	2587 (5.3)	Subtotal splenectomy, multiple infarcts	1366 (35)
13	None	Mild	Abnormal signal, post. rt. lobe	1140 (2.9)	Nodules and infarcts	2022 (67.5)
14	Plana: T10 Partial: T5, T12	Mild	Heterogeneous texture	1626 (3.2)	Extensive infarction calcification	2322 (56.9)
15	None	Mild	Enlarged only	1918 (4.1)	Extensive infarction	3692 (97.7)
16	Plana: T5–7, T9, T11 Partial: T3, T12, L4/kyphosis	Severe	Enlarged only	1133 (2.1)	Removed	
17	Normal	None	Abnormal signal post. rt. lobe	744 (2.7)	Enlarged but homogeneous	419 (18.7)

[a] Autopsy findings: liver, marked infiltration with Gaucher cells and fibrosis; generalized lymphadenopathy; bone marrow and adrenal glands filled with Gaucher cells

[b] Autopsy findings: liver, marked infiltration with Gaucher cells, regenerating nodules, fibrosis; abdominal lymph nodes, bone marrow and spleen filled with Gaucher cells

[c] Autopsy findings: liver, few Gaucher cells, extensive bridging fibrosis and regenerating nodules; occasional Gaucher cells in spleen, thymus, mesenteric and mediastinal nodes

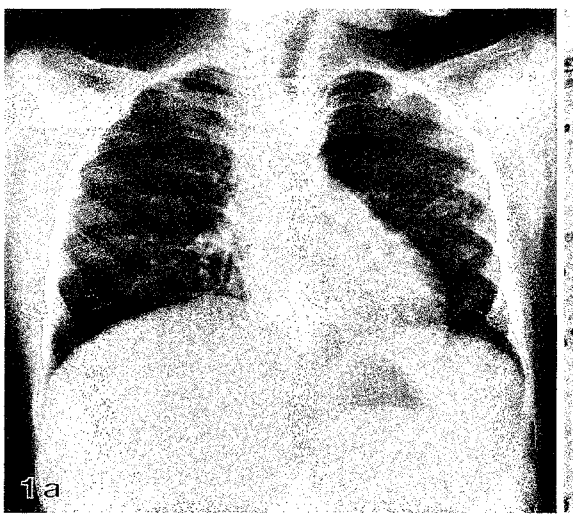

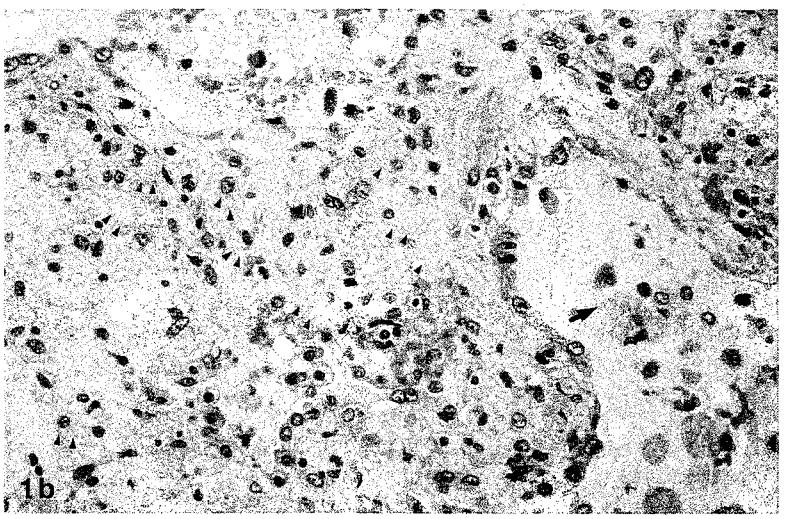

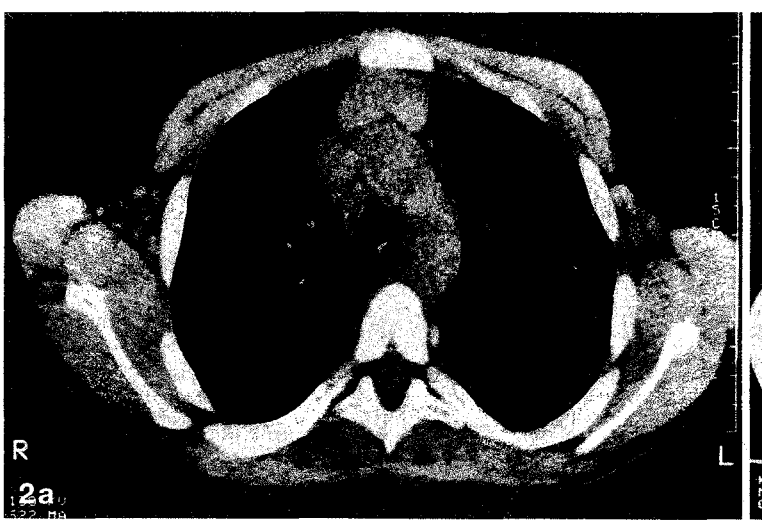

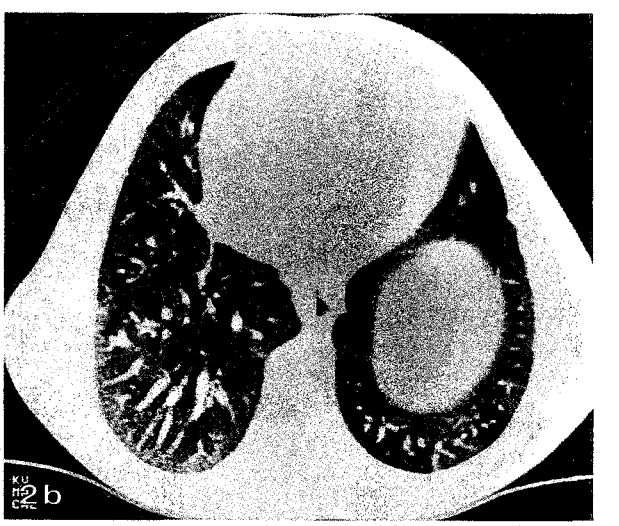

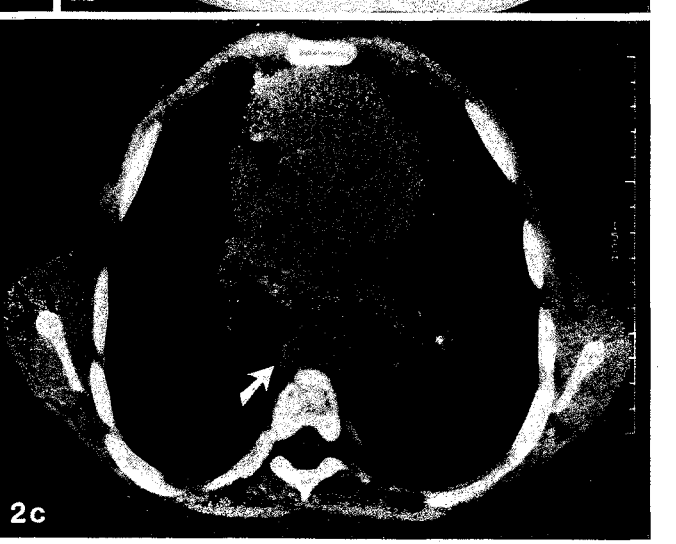

Fig. 1a, b Patient 6. **a** Posteroanterior chest radiograph of a 15-year-old girl demonstrates perihilar interstitial infiltrates. **b** Micrograph of lung shows heavy infiltration of Gaucher cells in the interstitium *(arrowheads)* between two alveoli which contain a few macrophages *(arrow)*. Hematoxylin-eosin stain, original magnification × 600

Fig. 2a, b Patient 12. **a** Transaxial CT image of a 9-year-old boy demonstrates a prominent thymus and bilateral axillary lymphadenopathy. **b** Bilateral lung abnormalities with pattern suggesting both interstitial and alveolar components. **c** Enlarged azygos vein *(arrow)* suggesting collateral circulation due to cirrhosis of the liver. Increased anteroposterior diameter of the chest is noted due to thoracic kyphosis

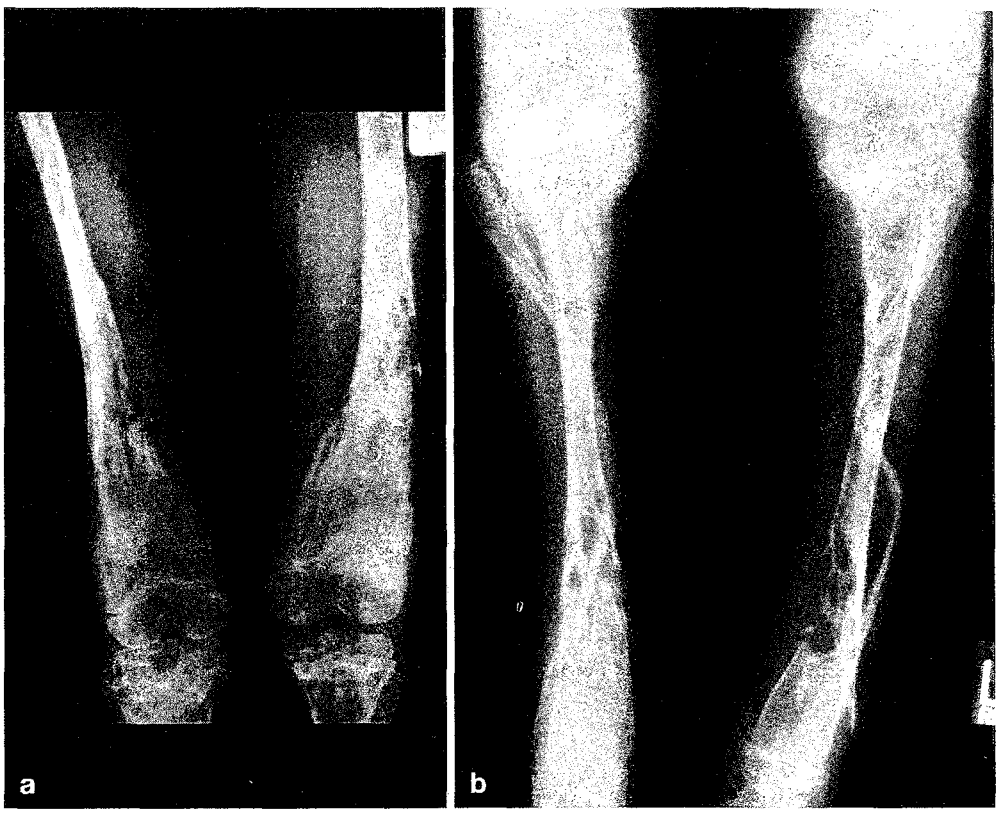

Fig. 3 a, b Patient 5. Anteroposterior radiographs of **a** the femurs and **b** the tibias and fibulae of a 15-year-old boy demonstrate severe bone changes with Erlenmeyer flask deformities, cystic changes with cortical erosions and a twisted, ribbon-like appearance of the fibulae

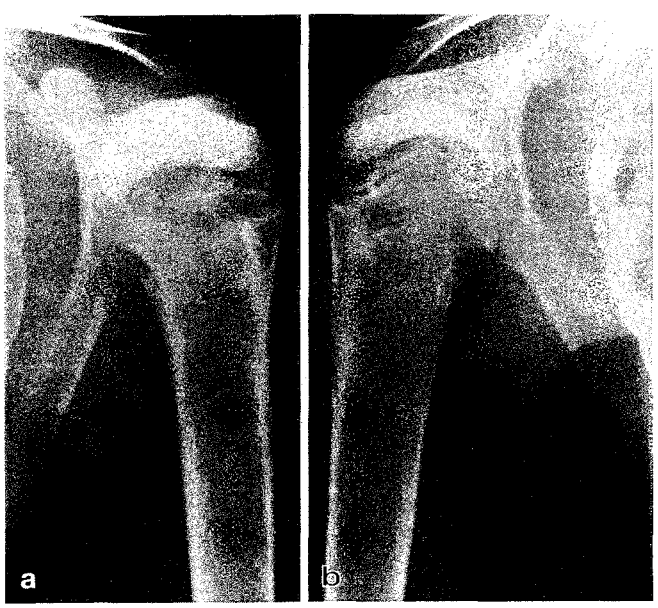

Fig. 4 a, b Patient 12. Anteroposterior radiograph of both humeri of a 13-year-old boy demonstrates erosions of the medial proximal cortex that are far more severe than normal

Autopsy findings

Nine patients died from hepatic, pulmonary or cardiac complications of the disease. Autopsies were performed on three of these patients. The autopsy was complete in two (patients 6 and 9), whereas in one it was limited to the brain, liver and mediastinum (patient 11).

Thorax

The thymus was examined in two patients and showed Gaucher cell infiltration in one (patient 9) and hyperplasia with occasional Gaucher cells in the other (patient 11). Generalized mediastinal and hilar lymphadenopathy secondary to Gaucher cell infiltration was noted in all three patients, and cervical lymphadenopathy was noted in one (patient 6). In the two patients in whom the lungs were examined, marked infiltration of Gaucher cells was seen in the interstitium in one (patient 6, Fig. 1 b) and a few Gaucher cells in the alveolar spaces were noted in the other (patient 9). Both patients with complete autopsies showed Gaucher cell infiltration in the myocardium and the intima and media of the aorta.

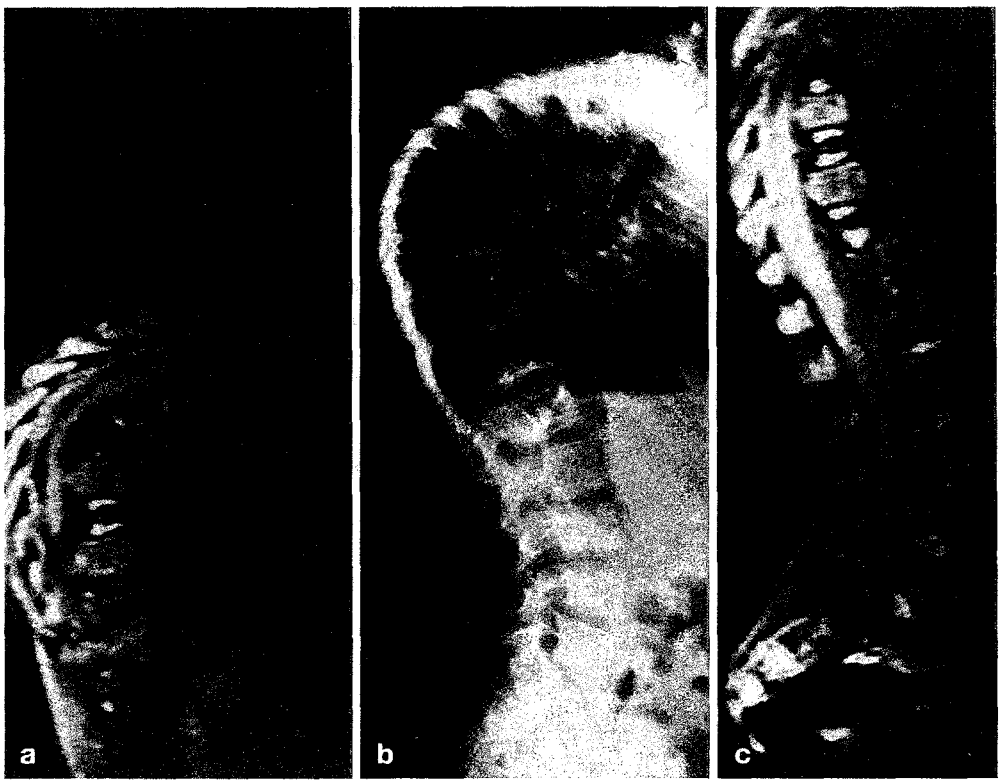

Fig. 5a–c Patient 16. Sagittal STIR MR scans (**a, c**) and lateral thoracolumbar radiograph (**b**) of a 9-year-old boy demonstrate multiple vertebra plana and severe thoracic kyphosis

Bone marrow

Samples of the vertebral bodies of two patients with complete autopsies showed complete replacement of the marrow fat by Gaucher cells.

Abdomen

The adrenal glands were examined in one patient and were of normal size, but showed Gaucher cell infiltration in the medulla (patient 6). Generalized mesenteric lymphadenopathy was present in all three patients. Numerous Gaucher cells were noted within the subcapsular and trabecular sinuses. The liver was examined in three patients. Marked infiltration with Gaucher cells along with fibrosis was noted in patients 6 and 9. In patient 11, numerous regenerating nodules mostly measuring approximately 0.3–0.4 cm in diameter were noted, with the largest one measuring 1.5 cm. There was extensive bridging portal fibrosis and mild hepatocellular necrosis. Abundant Gaucher cells were present in the spleen; the capsule was thickened and fibrous with vascular congestion and lymphocyte depletion of the white pulp.

Brain

Multiple sections of the brain showed small nodular accumulations of Gaucher cells in the perivascular spaces of the subcortical white matter of the parietal, temporal and occipital lobes. There were no Gaucher cells in the basal ganglia, thalamus, pons or cerebellum. There was no evidence of neuronophagia, which is prominent in patients with types 2 and 3a Gaucher disease [4].

Discussion

In 1882, Phillipe C. E. Gaucher, a French dermatologist, reported a female patient with an enlarged spleen that contained large unusual cells, which he believed to be an epithelioma [10]. The eponym, "Gaucher disease" was applied to this condition and the term Gaucher cell became commonly used to describe the characteristic engorged cells in their organs. In 1901, Brill suggested that Gaucher disease was familial [11], and later he recognized extension of the process beyond the spleen with involvement of the liver, lymph nodes and bone [12]. It was soon realized that Gaucher disease varied greatly in its age of onset, clinical manifestations and severity.

In 1961, Knudson and Kaplan [13] proposed a clinical classification of Gaucher disease that is still widely ac-

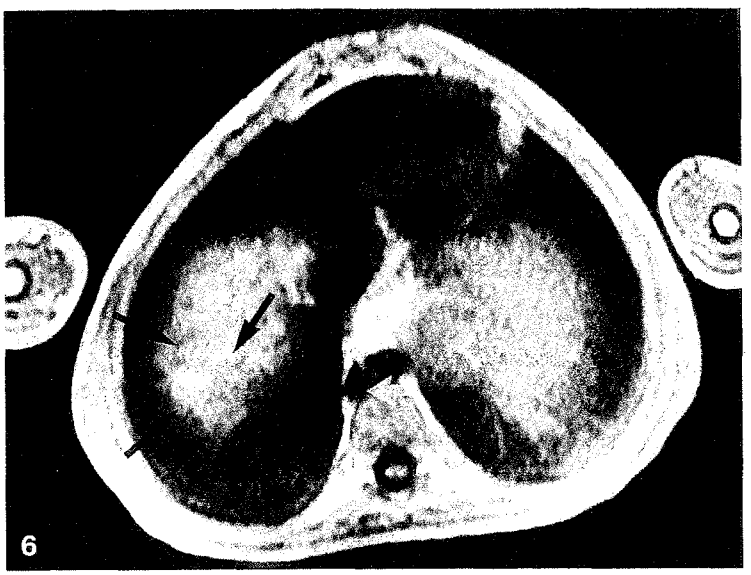

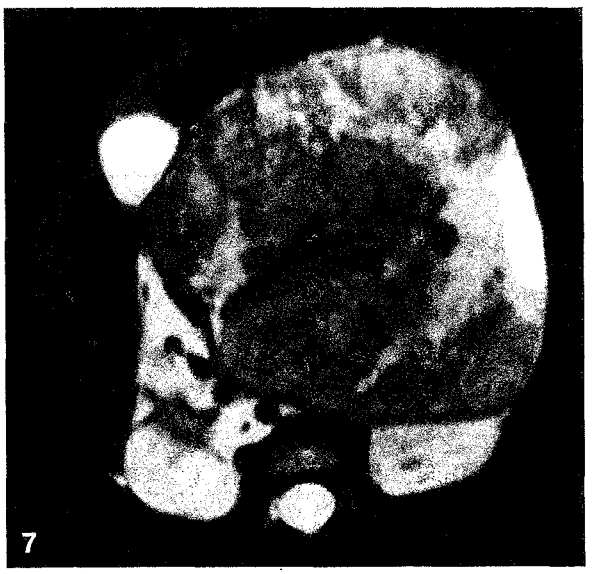

Fig. 6 Patient 11. Transaxial T1-weighted MR scan of the liver of an 8-year-old boy demonstrates hepatomegaly with several hyperintense regenerating nodules *(arrows)* and an enlarged azygos vein *(white arrow)*

Fig. 7 Patient 7. Transaxial T2-weighted MR scan of the liver and spleen of a 4-year-old boy demonstrates splenomegaly with a large, stellate area of subcapsular infarction

cepted. They designated type 1 Gaucher disease as a chronic visceral form of the disorder that spares the CNS, whereas the latter is involved to a variable extent in patients with types 2 and 3 disease. All three phenotypes of Gaucher disease are inherited as an autosomal recessive disorder and are caused by deficiency of the lysosomal enzyme glucocerebrosidase. The structural gene for this enzyme is located on chromosome 1q21–23, and over 50 mutations have been identified within it [14, 15].

The radiographic manifestations of type 1 Gaucher disease are well known [8, 16–19]. Data presented here reveal a similar distribution of abnormalities in patients with type 3b Gaucher disease. However, the findings are much more extensive and severe in the latter population and exhibit several distinctive features.

Patients with type 3b have a much shorter life expectancy than those with type 1 Gaucher disease. Nine of our 17 patients (53 %) died in childhood or adolescence from complications of aggressive systemic disease. Hepatosplenomegaly was pronounced, and hepatic failure with portal hypertension and bleeding esophageal varices was the most common cause of death (7/9). Pulmonary involvement is rare in type 1 Gaucher disease [20–22], but was common in our series of type 3b patients. Respiratory failure from interstitial fibrosis of the lungs was the second most common cause of death (2/9). Parenchymal infiltrates, some of which had a ground glass appearance, were observed in more than 50 % of our patients. These radiographic findings were due to accumulation of Gaucher cells in the interstitium and alveolar spaces, as shown at autopsy in two patients. Although histologic involvement of lymph nodes is frequent in patients with type 1 Gaucher disease, visible enlargement is not characteristic. In contrast, thoracic lymphadenopathy and thymic enlargement were readily apparent on CT of the chest in our type 3b patients.

Changes on plain radiographs of the long bones were common and frequently disabling in our patients with type 3b Gaucher disease (14/17). Although erosion of the medial cortex of the proximal humerus may be seen rarely in normal children and in patients with conditions such as Niemann-Pick disease (23), leukemia (24), or metastatic disease, this finding was present in 50 % of our patients with type 3b Gaucher disease. Vertebral compression fractures were also much more frequent in the latter patients, especially in the thoracolumbar area, where an incidence of 73 % was observed, compared with 24 % in type 1 Gaucher disease (S. C. Hill and N. W. Barton unpublished data, 41 patients, age 2–70 years). A single vertebra was involved in 18 % of cases and multiple levels in 82 %; involvement of multiple vertebrae frequently led to severe kyphosis.

Predictably, since the neurological abnormalities in patients with type 3b Gaucher disease are subtle, the CNS imaging findings were minimal. This is most readily explained by the sparse Gaucher cell infiltrate observed pathologically in the brain in this phenotype [5]. We observed only a minor degree of cerebral atrophy in four of our cases. One patient showed an abnormal signal intensity in the cerebral white matter that was most likely related to an episode of asphyxia in infancy, independent of Gaucher disease.

In summary, although types 1 and 3b Gaucher disease share the same spectrum of radiographic findings, the manifestations are more severe in the latter. Pulmonary infiltrates, thoracic lymph node enlargement, vertebral compression fractures and osteonecrosis of the long bones occur much more frequently in patients with type 3b disease. Awareness of these radiographic features may facilitate early recognition of this aggressive phenotype of Gaucher disease and prompt therapeutic intervention [6].

Acknowledgement We would like to thank Dr. Tom Giordano for his assistance in the pathology review of case 11.

References

1. Brady RO, Kanfer JN, Shapiro D (1965) Metabolism of glucocerebrosides: evidence of an enzymatic deficiency in Gaucher disease. Biochem Biophys Res Commun 18: 221–225
2. Barranger JA, Ginns EI (1989) Glucosylceramide lipidoses: Gaucher disease. In: Scriver CR, Beaudet AL, Sly WS, Valle D (eds) The metabolic basis of inherited disease, 6th edn. McGraw-Hill, New York, pp 1677–1698
3. Erickson A (1986) Gaucher disease-Norrbottnian type (III): neuropediatric and neurobiological aspects of clinical patterns and treatment. Acta Paediatr Scand [Suppl] 362: 1–42
4. Winkleman MD, Banker BQ, Victor M, Moser HW (1983) Non-infantile neuronopathic Gaucher's disease: a clinicopathologic study. Neurology 33: 994–1008
5. Patterson MC, Horowitz M, Abel RB, et al (1993) Isolated horizontal supranuclear gaze palsy as a marker of severe systemic involvement in Gaucher disease. Neurology 43: 1993–1997
6. Barton NW, Brady RO, Dambrosia JM, et al (1991) Replacement therapy for inherited enzyme deficiency: macrophage-targeted glucocerebrosidase for Gaucher disease. N Engl J Med 324: 1464–1470
7. Rosenthal DI, Doppelt SH, Mankin HJ, et al (1995) Enzyme replacement therapy for Gaucher disease: skeletal responses to macrophage-targeted glucocerebrosidase. Pediatrics 96: 629–637
8. Hill SC, Damaska BM, Ling A, et al (1992) Gaucher disease: abdominal imaging findings in 46 patients. Radiology 184: 561–566
9. Kita K, Kita M, Sato M, Ooshima A, Yamada R (1996) MR imaging of liver cirrhosis. Acta Radiologica 37: 198–203
10. Gaucher PCE (1882) De l'epithelioma primitif de la rate. Thesis, University of Paris
11. Brill NE (1901) Primary splenomegaly with a report of three cases occurring in one family. Am J Med Sci 21: 377–392
12. Brill NE (1904) A case of "splenomegalie primitif" with involvement of the haemopoietic organs. Proc NY Pathol Soc 4: 143–149
13. Knudson AG, Kaplan WD (1962) Genetics of the sphingolipidoses. In: Aronson SM, Volk BW (eds) Cerebral sphingolipidoses. Academic Press, New York, pp 395–411
14. Brady RO, Barton NW, Grabowski GE (1993) The role of neurogenetics in Gaucher's disease. Arch Neurol 50: 1212–1224
15. Beutler E (1993) Gaucher disease as a paradigm of current issues regarding single gene mutations of humans. Proc Natl Acad Sci USA 90: 5384–5390
16. Stowens DW, Teitelbaum SL, Kahn AJ, Barranger JA (1985) Skeletal complications of Gaucher disease. Medicine 64: 310–322
17. Hill SC, Reinig JW, Barranger JA, et al (1986) Gaucher disease: sonographic appearance of the spleen. Radiology 160: 631–634
18. Glass RBJ, Poznanski AK, Young S, Urban MA (1987) Gaucher disease of the liver: CT appearance. Pediatr Radiol 17: 417–418
19. Rosenthal DI, Barton NW, McKusick KA, et al (1992) Quantitative imaging of Gaucher disease. Radiology 185: 841–845
20. Wolson AH (1975) Pulmonary findings in Gaucher's disease. Am J Roentgenol Radium Ther Nucl Med 123: 712–715
21. Hainaux B, Christophe C, Hanquinet S, Perlmutter N (1992) Gaucher disease: plain radiography, US, CT and MR diagnosis of lung, bone and liver lesions. Pediatr Radiol 22: 78–79
22. Tunaci A, Berkman YM, Gorkmen E (1995) Pulmonary Gaucher's disease: high resolution computed tomographic features. Pediatr Radiol 25: 237–238
23. Lachman R, Crocker A, Schulman J, Strand R (1973) Radiological findings in Niemann-Pick disease. Radiology 108: 659–664
24. Melhem RE, Saber TJ (1980) Erosion of the medial cortex of the proximal humerus. Radiology 137: 77–79